Hindawi
Advances in Meteorology
Volume 2019, Article ID 6324878, 12 pages
https://doi.org/10.1155/2019/6324878

Research Article

Spatiotemporal Changes and Frequency Analysis of Multiday Extreme Precipitation in the Huai River Basin during 1960 to 2014

Yixing Yin[1], **Xin Pan**[2], **Xiuqin Yang**[1], **Xiaojun Wang**[3], **Guojie Wang**[4] and **Shanlei Sun**[1]

[1]*School of Hydrology and Water Resources, Nanjing University of Information Science and Technology, Nanjing 210044, China*
[2]*Quzhou Meteorological Administration, Quzhou 324000, China*
[3]*State Key Laboratory of Hydrology-Water Resources and Hydraulic Engineering, Nanjing Hydraulic Research Institute, Nanjing 210029, China*
[4]*School of Geographical Sciences, Nanjing University of Information Science and Technology, Nanjing 210044, China*

Correspondence should be addressed to Yixing Yin; yyxrosby@126.com

Received 14 January 2019; Revised 23 April 2019; Accepted 9 July 2019; Published 14 August 2019

Academic Editor: Harry D. Kambezidis

Copyright © 2019 Yixing Yin et al. This is an open access article distributed under the Creative Commons Attribution License, which permits unrestricted use, distribution, and reproduction in any medium, provided the original work is properly cited.

Floods and droughts are more closely related to the extreme precipitation over longer periods of time. The spatial and temporal changes and frequency analysis of 5-day and 10-day extreme precipitations (PX5D and PX10D) in the Huai River basin (HRB) are investigated by means of correlation analysis, trend and abrupt change analysis, EOF analysis, and hydrological frequency analysis based on the daily precipitation data from 1960 to 2014. The results indicate (1) PX5D and PX10D indices have a weak upward trend in HRB, and the weak upward trend may be due to the significant downward trend in the 21st century, (2) the multiday (5-day and 10-day) extreme precipitation is closely associated with flood/drought disasters in the HRB, and (3) for stations of nonstationary changes with significant upward trend after the abrupt change, if the whole extreme precipitation series are used for frequency analysis, the risk of future floods will be underestimated, and this effect is more pronounced for longer return periods.

1. Introduction

According to the IPCC's fifth assessment report, from 1880 to 2012, the global average surface temperature has risen by 0.85°C, and global warming has become an undisputed fact. Due to global warming, the water cycle has intensified, leading to frequent weather and climatic events such as heat waves, drought, and heavy precipitation. Extreme weather and climate events have become a focus for many scholars in recent years because of their suddenness and great harm to human lives and property. Both the intensity and occurrence frequency of extreme precipitation have been changing with upward/downward trends in different regions of the world [1–5]. In recent years, many researchers have also studied the extreme precipitation in China and have achieved a lot of results. Zhai et al. [6] tested on the trend of extreme precipitation in China and found that there was no obvious change in annual precipitation in China as a whole, and the precipitation intensity showed an upward trend, but the trend of extreme precipitation events showed obvious spatial differentiation.

The hydrological elements have changed a lot in response to the global climate change in the Huai River basin (HRB) [7–10]. The extreme precipitation events in this region have also become one of the hot topics of scholars in hydrology and meteorology. Xia et al. [11] showed that most of the maximum precipitation events concentrated in the 1960s~1970s, most of which occurring in the flood season, and the maximum daily precipitation increased in the HRB during the period from 1960 to 2009. Lu et al. [12] found that the precipitation events tended to be more extreme in 1960–2008 in the HRB. Yang and Cheng [13] found that the

number of extreme precipitation days, the amount of extreme precipitation, and its percentage in the total amount of Meiyu rainfall all showed a significant upward trend. Wang et al. [14] indicated that the probability of extreme precipitation from May to September increases in 1961–2011 in most areas of the Yangtze-Huai regions. Rong et al. [15] demonstrated that extreme precipitation is stronger in the semihumid region of the HRB, while it is less extreme in the humid zone.

Frequency analysis reveals the statistical characteristics of hydrological stochastic series and gives quantitative prediction of possible long-term changes of hydrological series in the sense of probability (e.g., return levels and return periods). Therefore, frequency analysis can provide some important information about the risk of flood disasters in a region. However, in hydrological frequency analysis, if the hydrological series are nonstationary (e.g., with significant trends or abrupt changes), the nonstationarity will have an important impact on the estimated return levels of extreme precipitation and runoff further influencing the assessment of flood risk [16, 17]. Under the background of global change, the stationarity of hydrological series has been destroyed to a certain degree [18], and we will face more nonstationarity in the future. How the nonstationarity in extreme precipitation and runoff series exert impacts on the estimation of return levels? This problem still needs to be investigated.

In the context of the interdecadal changes of the East Asian summer monsoon, there have been many north-south migrations in the rain belt in eastern China since the 1950s [19]. For example, in the 1980s, the rain belt was mainly located in the middle and lower reaches of the Yangtze River, and it has also experienced an interdecadal northward shift after the 1990s, showing an increase in summer precipitation in the HRB [20]. In this context, it is very important to reexamine the characteristics of extreme precipitation in the HRB using updated precipitation data. Floods and droughts are more closely related to extreme precipitation over longer periods of time (e.g., multiday extreme precipitation), which has not been studied sufficiently so far. In this paper, the temporal and spatial changes and frequency analysis of 5-day and 10-day extreme precipitations in the HRB are explored by trend analysis, ARCGIS spatial analysis, EOF analysis, and hydrological frequency analysis.

2. Data and Methods

2.1. Data. The data in this paper are derived from the precipitation observation data set provided by the National Meteorological Information Center. The National Meteorological Information Center has carried out strict quality control of the data, such as correcting some suspicious/false observations and correcting some data heterogeneity that may be caused by site migration and observation equipment upgrades. The data selected in this paper are the daily precipitation data of 47 sites in the HRB from 1960 to 2014. The European Commission-funded project Statistical and Regional Dynamical Downscaling of Extremes for European Regions (STARDEX) was carried out to enhance the methods for downscaling extreme temperature and precipitation from GCM [21, 22]. Floods and droughts are more closely related to extreme precipitation over longer periods of time. Therefore, the annual maximum 5-day and 10-day precipitations, namely, the indices of PX5D and PX10D are selected in this study. They are calculated by using the software of STARDEX. The location of the selected stations is shown in Figure 1.

2.2. Methods

2.2.1. Empirical Orthogonal Analysis. The empirical orthogonal function (EOF) method has obvious advantages in extracting information of spatiotemporal changes of physical fields and has been an important method for meteorologists to analyze data [23, 24]. The EOF analysis method is as follows: all the data are arranged into an X matrix of n rows and m columns, where n is the number of meteorological stations and m is the observations of meteorological elements (each row represents the m observations of a meteorological station). The EOF method is to decompose the spatiotemporal data X into time vectors Z and space vectors V:

$$X = VZ, \tag{1}$$

where V is a matrix of n row and n column, each column represents a typical space field. Z is an n-row and m-column matrix, and each row represents the time-weighted coefficients relevant to corresponding column in V. The space vectors are orthogonal to each other:

$$V^{\mathrm{T}} \cdot V = I, \tag{2}$$

where I is a unit matrix. The time vectors are also orthogonal:

$$Z \cdot Z^{\mathrm{T}} = \Lambda, \tag{3}$$

where Λ is a diagonal matrix. V and Z can be derived from the matrix X after defining the matrix A as follows:

$$A = X \cdot X^{\mathrm{T}}. \tag{4}$$

The data will be processed as departure from the mean values of each station. Therefore, A is a covariance matrix and also a real matrix. According to the factorization theorem of real symmetric matrices, we have

$$A = V \Lambda V^{\mathrm{T}}, \tag{5}$$

where V is the eigenvector of A and also the space vector of X and Λ is the diagonal matrix of A whose principal diagonal is the eigenvalue of A and the rest are all 0. Then the time vectors Z can be obtained as

$$Z = V^{\mathrm{T}} X. \tag{6}$$

2.2.2. Hydrological Frequency Analysis. In the hydrological frequency analysis, the linear moment method (L-moment) proposed by Hosking [25, 26] is adopted in the parameter

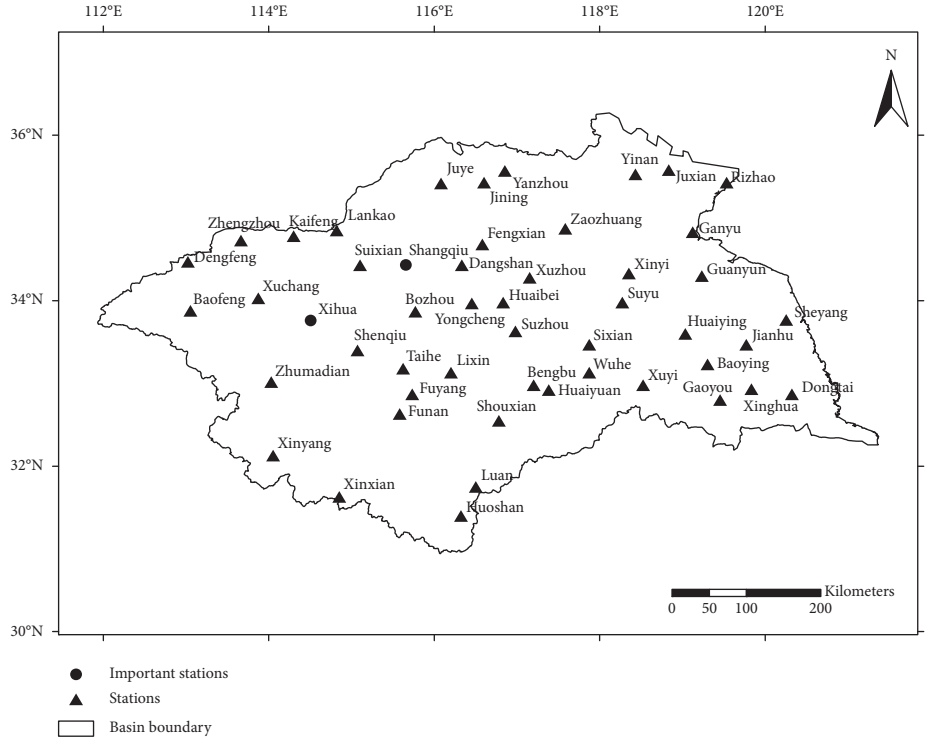

Figure 1: Distribution of meteorological stations in the Huai River basin (HRB). Xihua station and Shangqiu station are labled as "important stations," which will be used in the frequency analysis in Section 3.3.

estimation, and the unbiased sample moment estimation method is used in the calculation.

Let $X_{1:n} \le X_{2:n} \le \cdots \le X_{n:n}$ be the order statistics of a random sample of size n which is drawn from the distribution of X. Define the rth L-moment of variable X to be

$$\lambda_r \equiv r^{-1} \sum_{k=0}^{r-1} (-1)^k \binom{r-1}{k} EX_{r-k:r}, \quad r = 1, 2, \ldots, \tag{7}$$

where $EX_{r-k:r}$ is the $(r-k)$ th order statistics from a sample size of r.

The Weibull formula is used as the plotting position formula, which is given as [27]:

$$P_m = \frac{m}{n+1}, \tag{8}$$

where n is the sample size and m is the rank of the observations in the ascending order.

Candidate fitting distribution types include generalized extreme value distribution (GEV), Pearson type III distribution (P-III), three-parameter lognormal distribution (LN3), generalized logistic distribution (GLOG) distribution, value I-type distribution (EV1), generalized Pareto distribution (GPAR), Weibull distribution (Weibul), normal distribution (N), exponential distribution (EXP), logistic distribution (LOG), two-parameter lognormal distribution (LN2), gamma distribution (GAM), logarithmic Pearson type III distribution (LP-III), four-parameter Wakeby (wk4), and five-parameter Wakeby (wk5). The chi-square and Kolmogorov–Smirnov tests were used for the selection of distributions, which are described in detail by Rao and Hamed [28].

3. Results and Analysis

3.1. Temporal Changes of PX5D and PX10D. Figure 2 exhibits the Mann–Kendall trend of the PX5D and PX10D series during 1960–2014 in the HRB. For PX5D, more than half of the stations have positive trend, but only one station (Xihua Station) is significant at the 0.05 level, and the other (Wuhe Station) is significant at the 0.1 significance level. For PX10D, the results are quite similar: most of the stations have positive trends, with two stations (Xihua Station and Wuhe Station) significant at the 0.1 level. No stations with negative trend are significant at 0.05 or 0.1 level for the two indices. Therefore, in general, the PX5D and PX10D indices have a weak upward trend in the HRB.

The average PX5D and PX10D in the basin were quite similar to each other from 1960 to 2014 (Figure 3). And the correlation coefficient between them is up to 0.95. The linear fitting curves of them have an upward trend according to the regression coefficients, but not significant. The Mann–Kendall trend test also showed that there were no significant trends for them. However, linear fitting curves of the two indices after the year 2003 indicated that the downward trend of them during this period both reached a significance level of 0.05. Therefore, the significant decline of extreme precipitation in the twenty-first century leads to the overall increase of the two series to be nonsignificant.

Combined with the flood and drought damaged areas in the HRB from 1960 to 2000, it can be found that there is

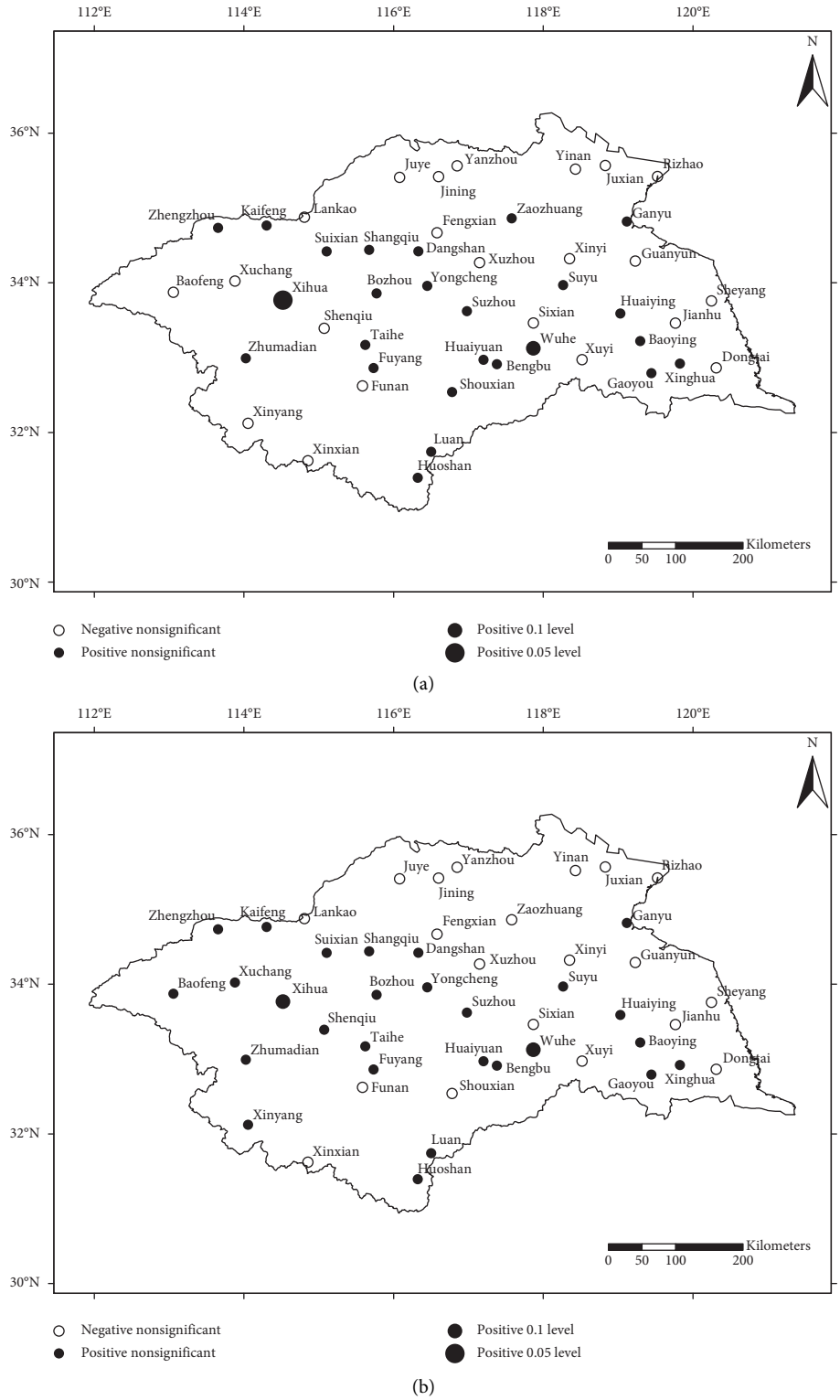

Figure 2: Spatial pattern of the Mann–Kendall trend of extreme precipitation indices of (a) PX5D and (b) PX10D in the HRB.

good correspondence between the peaks/valleys of PX5D/PX10D and the floods/droughts in the basin (Figure 4). The peaks and valleys of PX5D and PX10D are consistent with those of the flood areas in Figures 4(a) and 4(c), while the peaks and valleys of PX5D and PX10D are in reverse to those of the drought areas in Figures 4(b) and 4(d). The correlation coefficients between PX5D (PX10D) and flood and drought damaged areas are 0.50 (0.59) and −0.38 (−0.47) during the period from 1960 to 2000, respectively, all of which reaching 0.05 significant level. PX5D and PX10D were mainly at their

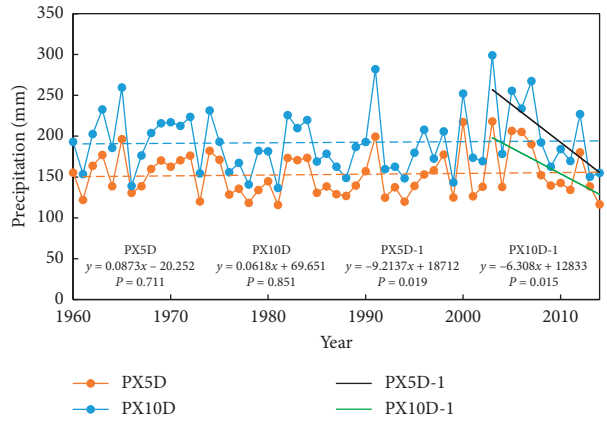

Figure 3: Changes of extreme precipitation indices of PX5D and PX10D in the HRB. Dashed lines indicate the linear trend of PX5D and PX10D, and black and green lines indicate the trends of PX5D and PX10D during the period between 2003 and 2014.

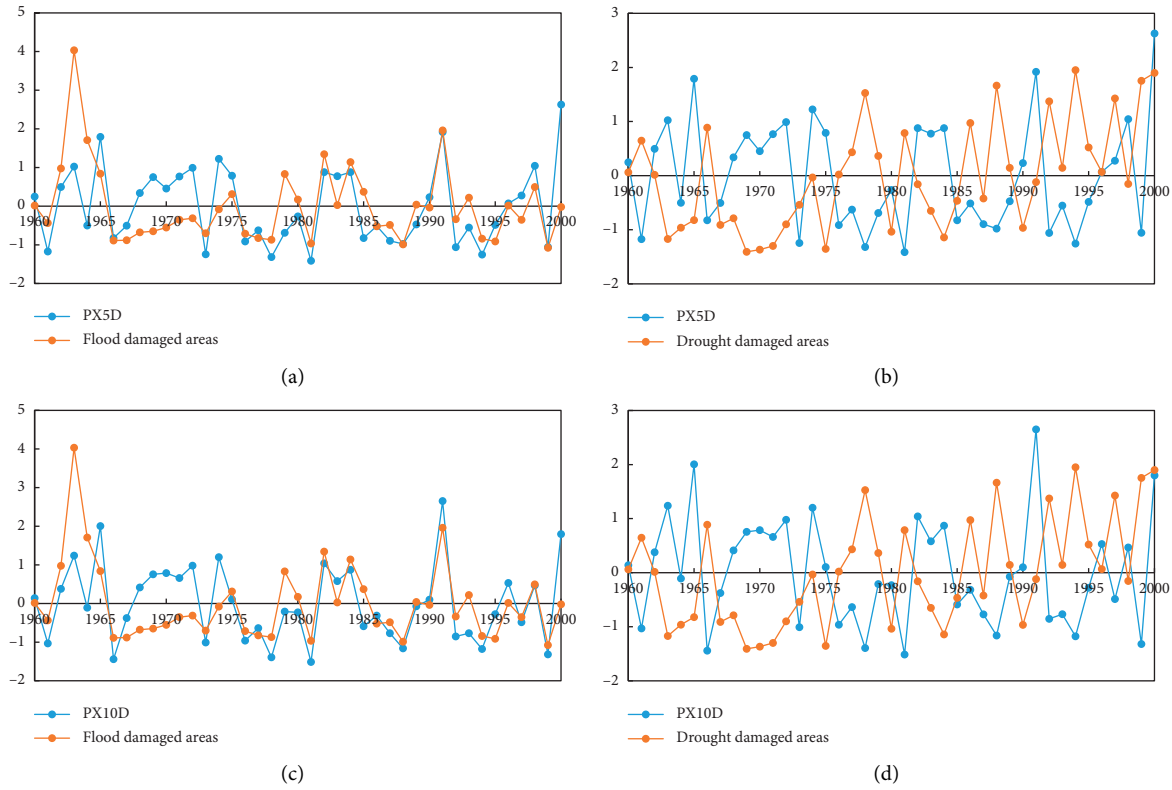

Figure 4: Relation between PX5D/PX10D and flood/drought damaged areas in the HRB (standardized series): (a, c) flood damaged areas (b, d) drought damaged areas.

peaks in the years when floods occurred (e.g., 1991, 2003, and 2007), and they were mainly at their valleys during the years with severe droughts (e.g., 1992, 1994, 1999, and 2001). Therefore, the changes of extreme precipitation are one of the major factors influencing floods and droughts in the HRB.

3.2. Spatiotemporal Patterns of PX5D and PX10D. Empirical orthogonal function (EOF) analysis is used to decompose the extreme precipitation into spatial and associated temporal patterns. The North test proposed by North et al. [29] is used to test whether the modes of EOF analysis are significant, and the results indicate that the first two modes of PX5D passed the North test. EOF results of PX5D are shown in Figure 5, and the results of PX10D (not shown) are very similar to PX5D. Figures 5(a) and 5(b) show the leading modes of PX5D in the HRB. EOF1 accounts for 20.93% of the total variance. From 5(a), it is found that the first mode has a loading which is almost entirely positive in the basin, and only some individual sites in the northwest are negative, reflecting the spatial consistency of PX5D. Besides, large values are concentrated over the mid- and southern parts of

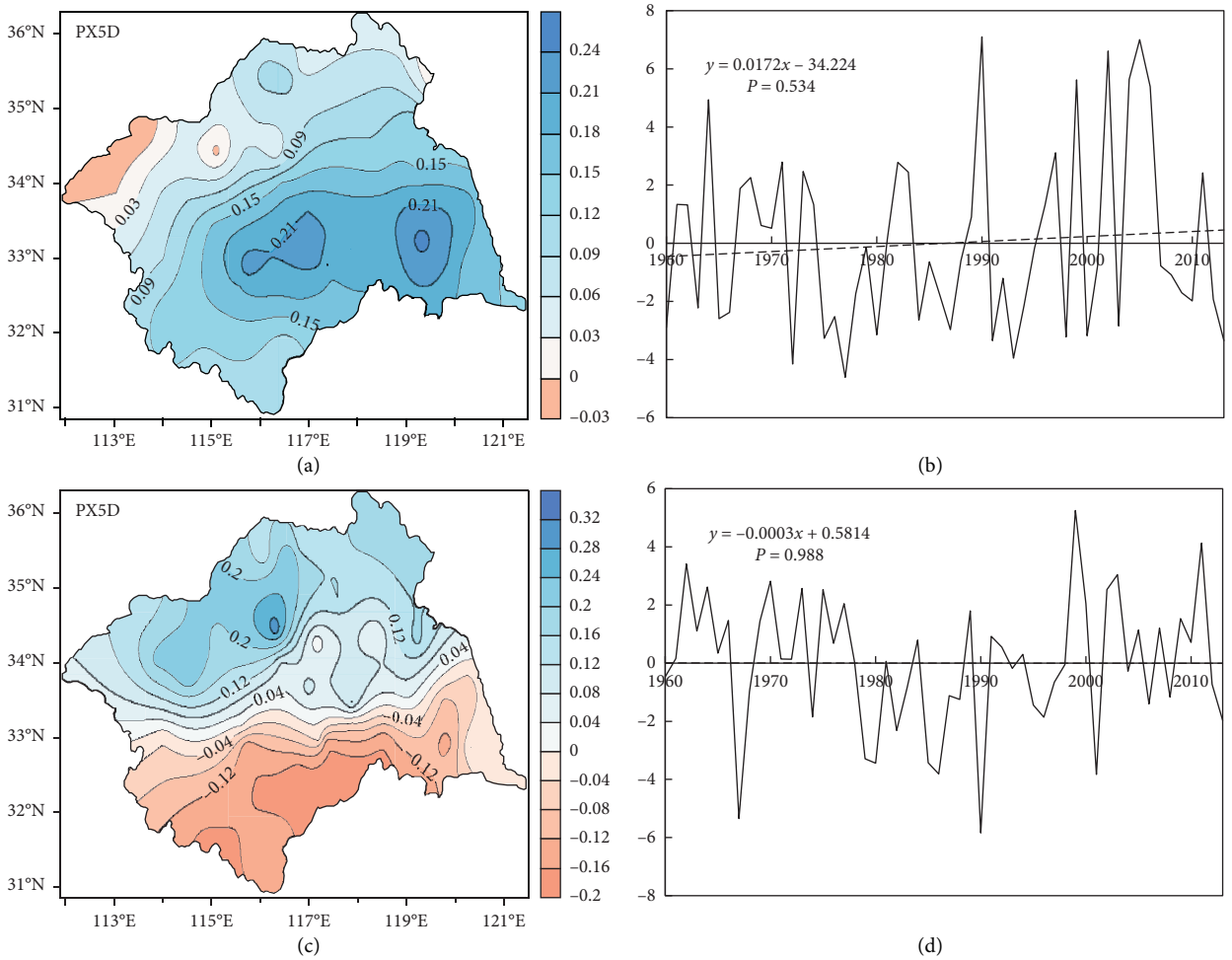

Figure 5: EOF results of PX5D in HRB. (a) EOF1. (b) PC1. (c) EOF2. (d) PC2.

the basin. The first principal component (PC1) has a weak upward trend, but not significant (Figure 5(b)), and this is similar to the trend of PX5D in Section 3.1. Combined with EOF1, 1990, 2001, and 2010 are the three years with the highest PX5D, and 1976, 1978 and 1993 are the years with the lowest PX5D.

Figures 5(c) and 5(d) are the EOF2 and the second principal component (PC2) of the PX5D. The percentage of variance explained by EOF2 is 11.21%. It can be found from 5(c) that there is a significant spatial difference between the north and the south. The northern part of the basin is dominated by negative values, and the southern part is positive, reflecting a meridional dipole pattern of PX5D. The downward trend of PC2 in Figure 5(d) is very weak.

Semenov and Bengtsson [30] pointed out that global warming will accelerate the water cycle, change the intensity and spatiotemporal distributions of precipitation, and increase the occurrence possibility of regional extreme precipitation events. PC1 of PX5D shows an upward trend, and this also confirms the viewpoint. Zhu et al. [31] demonstrated that the second eigenvector of precipitation in the Meiyu period exhibits the meridional dipole pattern in the region, which is consistent with the pattern of EOF2 in this paper. Their study also shows that the strength of East Asian subtropical summer monsoon, the position of west Pacific subtropical high, and the 200 hPa South Asian high are the main factors affecting the meridional dipole pattern. And the previous winter ENSO also has a certain impact on this kind of precipitation distribution. Further research still needs to be done to explore the mechanisms of the spatiotemporal patterns of extreme precipitation in the HRB.

3.3. Frequency Analysis of PX5D and PX10D. In this section, the effects of nonstationarity on the results of hydrological frequency analysis are explored utilizing the typical series of PX5D and PX10D with and without significant trends and abrupt changes in the HRB.

The Mann–Kendall trend and abrupt change test are used to detect the stationarity of the PX5D and PX10D series in the HRB, and most of the series do not have significant trend or abrupt changes. The trend test results of PX5D and PX10D are shown in Figure 3. The results of the abrupt change test of PX5D in Xihua Station and PX10D in Shangqiu are shown in Figure 6. As can be seen, PX5D was mainly in the negative phase from 1960s to 1990s and was in the positive phase after that, reaching the 0.05 significance

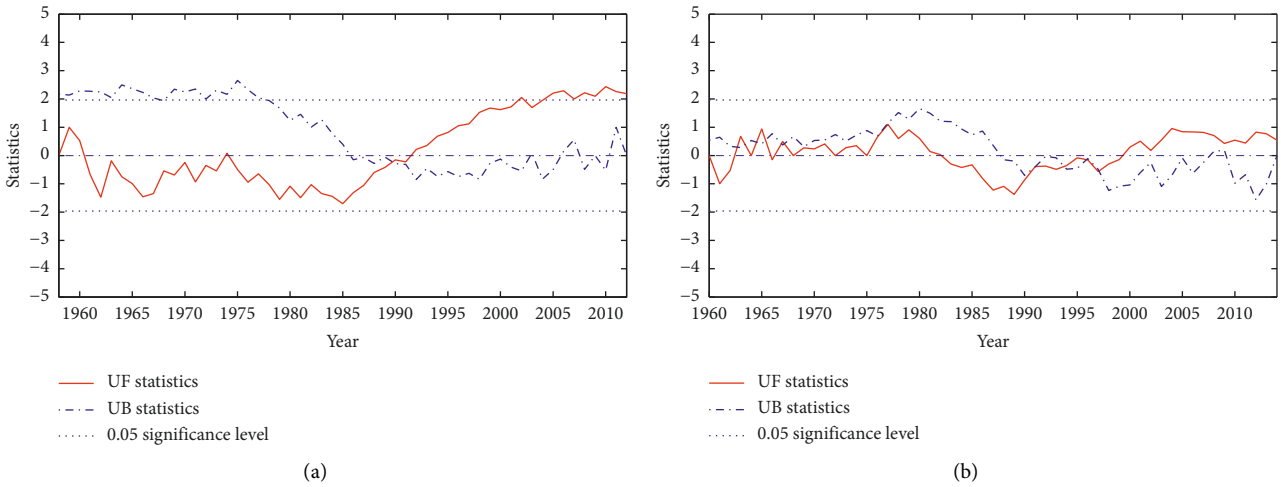

Figure 6: The Mann–Kendall abrupt change test of PX5D in Xihua (a) and PX10D in Shangqiu (b).

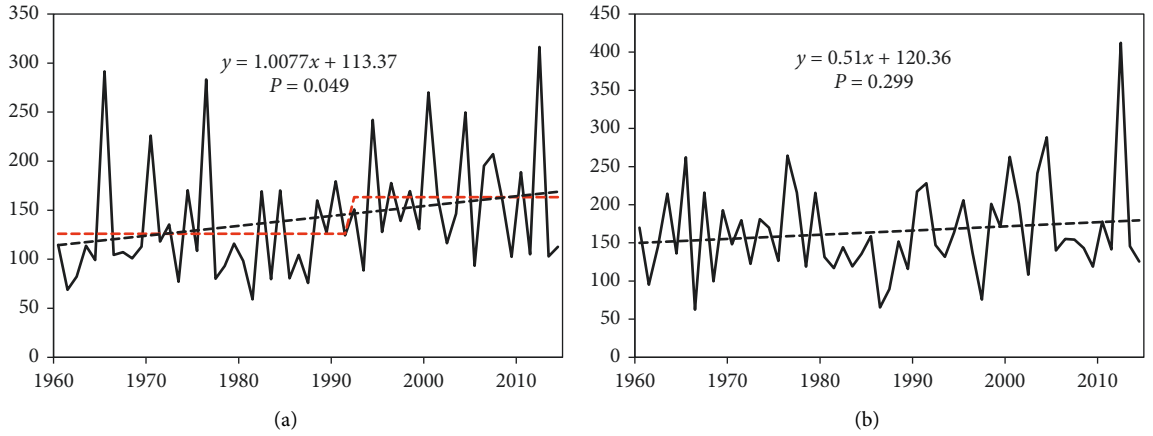

Figure 7: Time series of PX5D in Xihua (a) and PX10D in Shangqiu (b). The red dashed line shows the means of the subseries, and the black dashed lines show the linear trends.

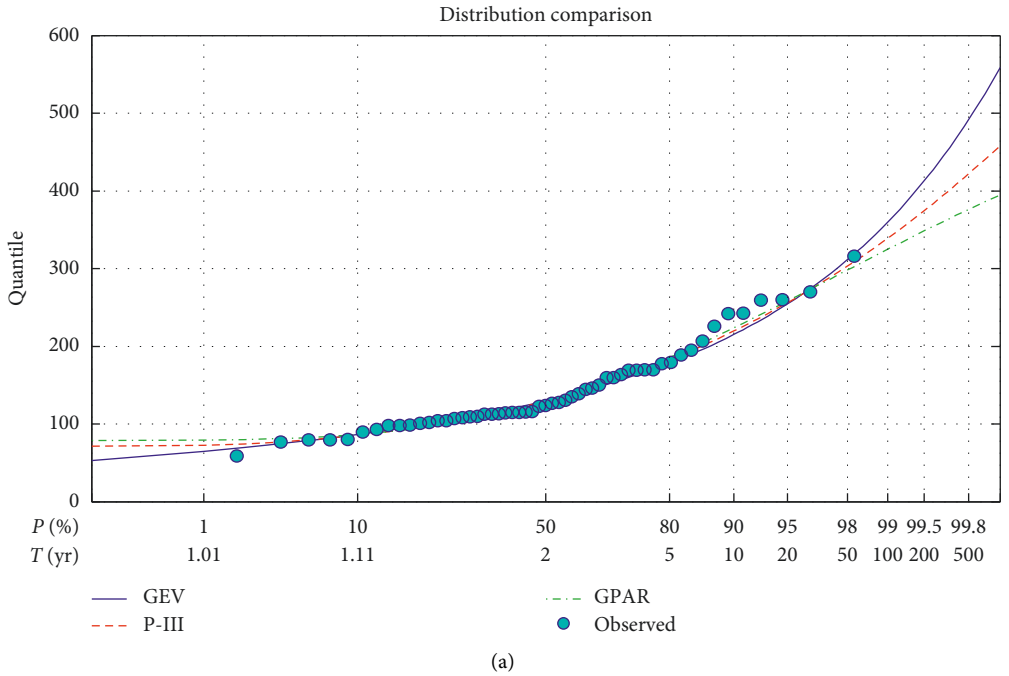

Figure 8: Continued.

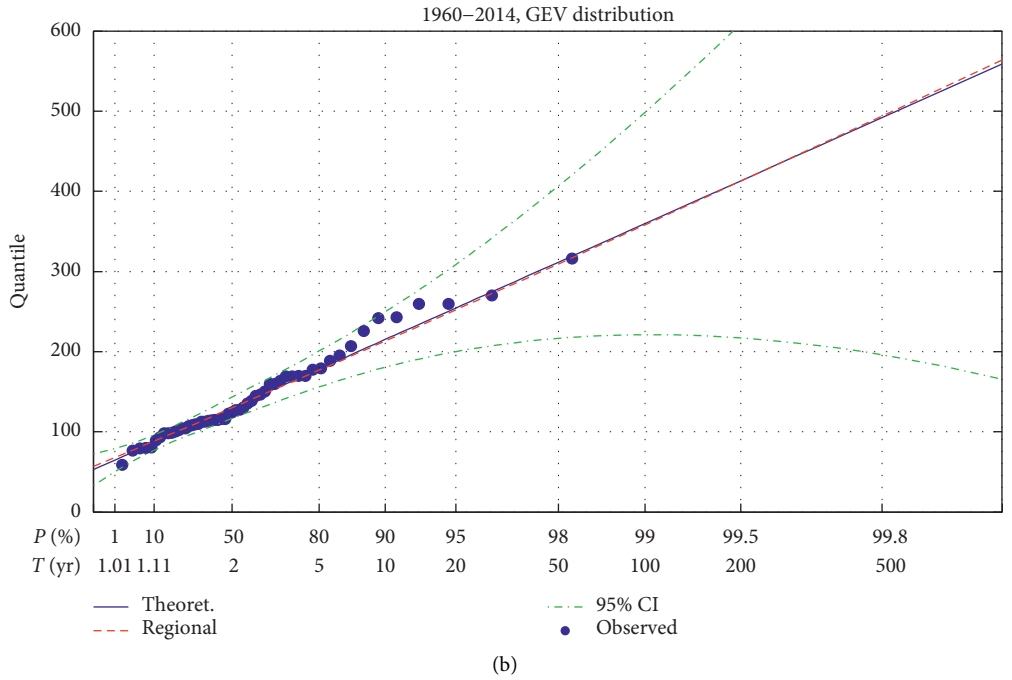

Figure 8: (a) Comparison of fitting curves of GEV, P-III, and GPAR. (b) Observed and estimated PX5D in Xihua station based on regional and at-site methods.

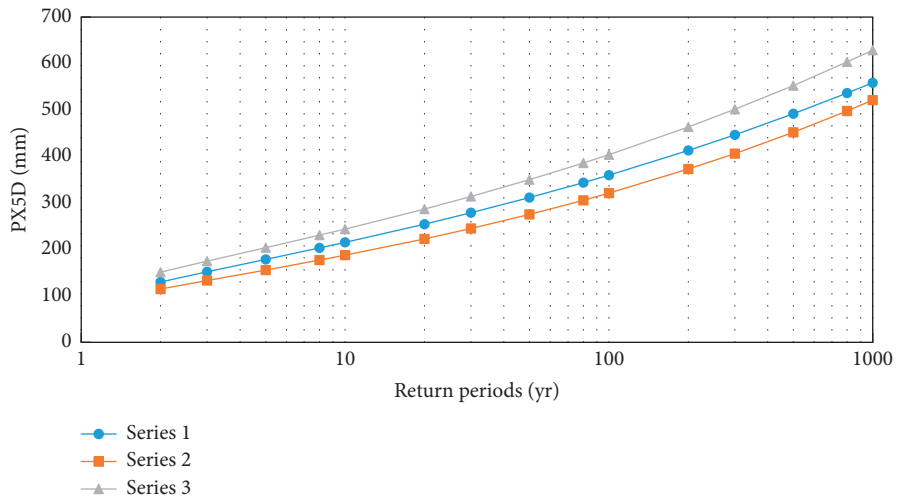

Figure 9: Frequency curves of the whole series (series 1), before (series 2), and after (series 3) the abrupt changes series of PX5D in Xihua station.

level in the middle and late 2000s. Judging from the UF and UB curves, the abrupt change occurred around 1991. The Z statistics of the Mann–Kendall trend test for the total series is 2.17; thus, the upward trend reached the 0.05 significance level. In a word, there is a significant trend and abrupt change in PX5D of Xihua Station, indicating that the series are nonstationary. In Figure 6(b), there is no abrupt change in PX10D of Shangqiu Station, and the Z statistics is only 0.54; thus, the PX10D series can be considered as stationary.

The original time series of PX5D in Xihua and PX10D in Shangqiu are shown in Figure 7. As can be seen, the linear upward trend of PX5D in Xihua is significant at the 0.05 level, and the mean values of the two subtime series (between 1960 and 1991 and between 1992 and 2014) are quite different. The average PX5D was low before 1991, but it was higher after 1991. And the PX10D series in Shangqiu are quite stationary, with no significant trend (but the year 2012 has an outlier).

The frequency analysis of PX5D in Xihua Station from 1960 to 2014 was first carried out. According to the goodness of fit test, GEV distribution was selected as the best distribution (at the 5% significance level based on both chi-square test and Kolmogorov–Smirnov test). Figure 8(a) gives the fitting result of GEV and compares the fitting curve of GEV with those of P-III and GPAR. It can be seen that the fitting of GEV distribution is better than the other

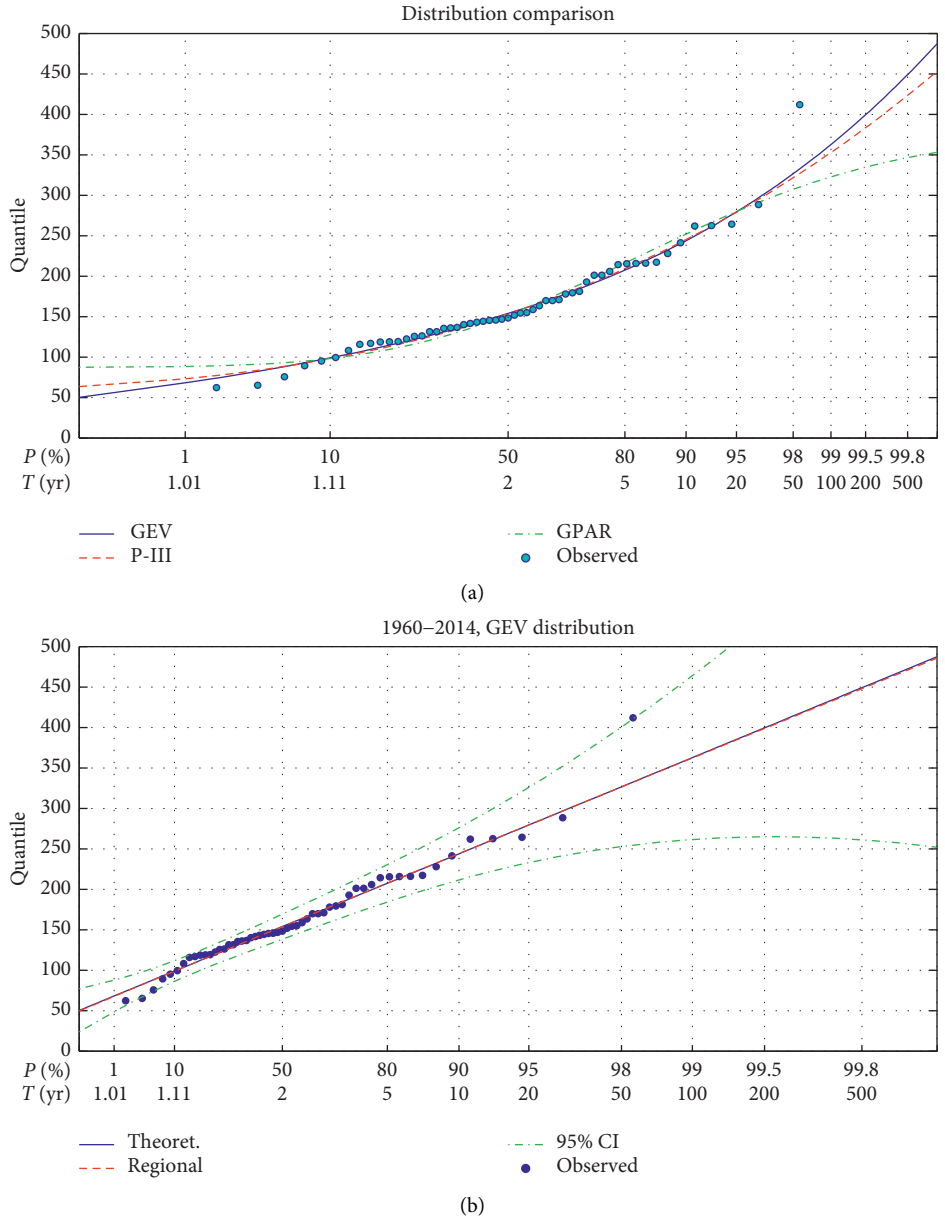

Figure 10: (a) Comparison of fitting curves of GEV, P-III, and GPAR. (b) Observed and estimated PX10D in Shangqiu Station based on regional and at-site methods.

two distributions. The observed and estimated PX5D based on regional and at-site methods is shown in Figure 8(b). The red line is the regional frequency curve (all the 47 stations in the study area are used as one homogeneous region). The blue line is the theoretical frequency curve which is based on the at-site method. And the red line and the blue line are very close to each other. It shows that all the observed points are close to the GEV curve, and the estimated values at the 5–20-year return periods are underestimated, but all the observed points are within the 95% confidence interval of the theoretical frequency curve. The GEV curve in Figure 8(b) is approximately a line, which is quite different from the GEV curve in Figure 8(a), and this is because the spacing of horizontal ordinate has changed in Figure 8(a).

PX5D series of Xihua Station was further divided into two subseries: series 2 (1961–1991) is before the abrupt change and series 3 (1992–2014) is after the abrupt change. And the whole series (1960~2014) is labeled as series 1. GEV is the best distribution for both series 1 and 2. Figure 9 is the estimated quantiles of PX5D for the three series at different return periods. As can be seen, the frequency curve of series 2 is significantly higher than that of series 1, and the curve of series 3 is located between the former two. Meanwhile, the differences between the estimation of series 1 and 2 increased with the increase of return periods. Therefore, the estimated quantiles (return levels) are small and unsafe when the analysis is based on series 1 or series 3. In addition, the Hurst index calculated by the R/S method is 0.91 for series 3 which indicates that PX5D of Xihua Station will increase in

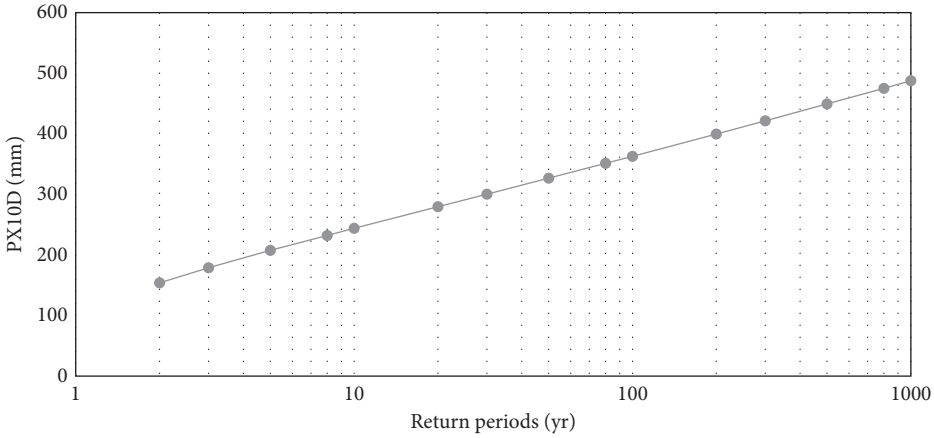

Figure 11: Frequency curve of PX10D in Shangqiu Station.

the future, and the extreme precipitation estimated by the whole series is even more unsafe.

The goodness of fit test indicated that GEV distribution is also the best distribution for PX10D in Shangqiu Station (at the 5% significance level for both chi-square and Kolmogorov–Smirnov test). Figure 10(a) gives the fitting result of GEV and compares the fitting curve of GEV with those of P-III and GPAR. The observed and estimated PX10D based on regional and at-site methods is shown in Figure 10(b). Besides, both Figures 10(a) and 10(b) have an outlier, which occurred in 2012. But all the observed points including the outlier are within the 95% confidence interval of the theoretical frequency curve in Figure 10(b).

Figure 11 shows the estimated quantiles (return levels) of PX10D in Shangqiu Station at different return periods. The return level of 100-year-PX10D is about 362.8 mm, and that of 50-year-PX10D is about 326.6 mm. The maximum PX10D in Shangqiu was 412.2 mm in 2012, which is up to a return period of nearly 300 years. The year with the second biggest PX10D is 2004 (PX10D is only 288.5 mm), and the return period is less than 30 years.

In the calculation of the quantiles of extreme precipitation, if the whole series is directly utilized in the frequency analysis and the stationarity test of the data series is neglected, two kinds of problems will occur: on the one hand, it does not meet the basic assumptions on data stationarity in frequency analysis; on the other hand, the estimated quantile is significantly different from those based on the series before or after the abrupt change, and this effect is more significant for longer return periods. The estimated extreme precipitation calculated according to the series after the abrupt change has higher accuracy, but this also increases the uncertainty of parameter estimation since the length (sample size) is significantly smaller than the whole series. In the future, when extreme precipitation continues to increase, the estimation by the whole series will be even more unsafe. Salas and Obeysekera [32] proposed a simple and unified framework to estimate the return period and risk for nonstationary hydrologic events. Gilleland and Katz [33] also proposed a GEV model based on nonstationary series recently. The estimated extreme precipitation changes with time and is known as "effective return level." However, how to apply the new methods to engineering hydrological design remains to be an open question [34, 35]. Therefore, frequency analysis of the nonstationary series needs to be studied in depth to obtain better estimation of extreme precipitation.

4. Conclusions

Floods and droughts are more closely related to extreme precipitation over longer periods of time. The spatial and temporal changes and frequency analysis of 5-day and 10-day extreme precipitations in the Huai River basin (HRB) are investigated by means of correlation analysis, trend and abrupt change analysis, EOF analysis, and hydrological frequency analysis based on the daily precipitation data from 1960 to 2014.

Generally, more stations have positive trends for PX5D and PX10D in the HRB. PX5D and PX10D indices have a weak upward trend in the HRB, and PC1 of the EOF analysis also has a weak upward trend. The weak upward trend may mainly be due to the significant downward trend in the 21st century.

The changes of PX5D and PX10D are well consistent with the flood and drought damaged areas in the basin. This indicates that the multiday (5-day and 10-day) extreme precipitation is closely associated with flood/drought disasters and can be used to study the risk of flood and drought in the future.

When the hydrological time series satisfy the stationarity consumption of frequency analysis, the series can be used without any changes. Nonstationary hydrological series with significant trends or abrupt changes will have important impacts in frequency analysis. For the stations with significant upward trend and abrupt changes, if the whole series are used for frequency analysis, the estimated quantiles will significantly be lower; thus, the risk of future flooding will be underestimated, and this effect will be more pronounced for longer return periods.

Data Availability

The data used to support the findings of this study are available from the corresponding author upon request.

Conflicts of Interest

The authors declare that they have no conflicts of interest.

Acknowledgments

This study was supported by the National Natural Science Foundation of China (41671022 and 41575094), Young Top-Notch Talent Support Program of National High-level Talents Special Support Plan, Strategic Consulting Projects of Chinese Academy of Engineering (2016-ZD-08-05-02), and Meteorological Research Foundation of the Huai River Basin (HRM201701).

References

[1] L. V. Alexander, X. Zhang, T. C. Peterson et al., "Global observed changes in daily climate extremes of temperature and precipitation," *Journal of Geophysical Research*, vol. 111, no. 5, article D05109, 2006.

[2] Y. Chen and P. M. Zhai, "Persistent extreme precipitation events in China during 1951–2010," *Climate Research*, vol. 57, no. 2, pp. 143–155, 2013.

[3] C. Onyutha, "Geospatial trends and decadal anomalies in extreme rainfall over Uganda, East Africa," *Advances in Meteorology*, vol. 2016, Article ID 6935912, 15 pages, 2016.

[4] Z. X. Zhang, Q. Jin, X. Chen, C.-Y. Xu, and S. S. Jiang, "On the linkage between the extreme drought and pluvial patterns in China and the large-scale atmospheric circulation," *Advances in Meteorology*, vol. 2016, Article ID 8010638, 12 pages, 2016.

[5] C. R. Balling Jr., M. S. K. Kiany, S. S. Roy, and J. Khoshhal, "Trends in extreme precipitation indices in Iran: 1951–2007," *Advances in Meteorology*, vol. 2016, Article ID 2456809, 8 pages, 2016.

[6] P. Zhai, X. Zhang, H. Wan, and X. Pan, "Trends in total precipitation and frequency of daily precipitation extremes over China," *Journal of Climate*, vol. 18, no. 7, pp. 1096–1108, 2005.

[7] Y. Wang, Q. Zhang, and V. P. Singh, "Spatiotemporal patterns of precipitation regimes in the Huai River basin, China, and possible relations with ENSO events," *Natural Hazards*, vol. 82, no. 3, pp. 2167–2185, 2016.

[8] G. Y. An and Z. C. Hao, "Variation of precipitation and streamflow in the upper and middle Huaihe river basin, China, from 1959–2009," *Journal of Coastal Research*, vol. 80, pp. 69–79, 2017.

[9] Z. Pan, X. Ruan, M. Qian, J. Hua, N. Shan, and J. Xu, "Spatio-temporal variability of streamflow in the Huaihe River Basin, China: climate variability or human activities?," *Hydrology Research*, vol. 49, no. 1, pp. 177–193, 2018.

[10] Z. W. Ye and Z. H. Li, "Spatiotemporal variability and trends of extreme precipitation in the Huaihe River Basin, a climatic transitional zone in East China," *Advances in Meteorology*, vol. 2017, Article ID 3197435, 15 pages, 2017.

[11] J. Xia, D. She, Y. Zhang, and H. Du, "Spatio-temporal trend and statistical distribution of extreme precipitation events in Huaihe River Basin during 1960-2009," *Journal of Geographical Sciences*, vol. 22, no. 2, pp. 195–208, 2012.

[12] Z. G. Lu, X. H. Zhang, J. L. Huo, K. Q. Wang, and X. P. Xie, "The evolution characteristics of the extreme precipitation in Huaihe river basin during 1960-2008," *Journal of the Meteorological Sciences*, vol. 31, no. 1, pp. 74–80, 2011, in Chinese.

[13] W. Yang and Z. Cheng, "Variation characteristics of extreme precipitation during Meiyu flood period over the Yangtze-Huaihe basin in recent 53 years," *Meteorological Monthly*, vol. 41, no. 9, pp. 1126–1133, 2015, in Chinese.

[14] J. Wang, J. H. Yu, and J. Q. He, "Study on characteristics and change trend of extreme rainfall in the Jianghuai region," *Climatic and Environmental Research*, vol. 20, no. 1, pp. 80–88, 2015, in Chinese.

[15] Y. S. Rong, W. Wang, P. Wang, and L. Y. Bai, "Analysis of characteristics of extreme rainfall and estimate of rainfall during return periods in Huaihe Basin," *Journal of Hohai University (Natural Sciences)*, vol. 40, no. 1, pp. 1–8, 2012, in Chinese.

[16] G. Villarini, J. A. Smith, F. Serinaldi, J. Bales, P. D. Bates, and W. F. Krajewski, "Flood frequency analysis for nonstationary annual peak records in an urban drainage basin," *Advances in Water Resources*, vol. 32, no. 8, pp. 1255–1266, 2009.

[17] A. T. Silva, M. M. Portela, and M. Naghettini, "Non-stationarities in the occurrence rates of flood events in Portuguese watersheds," *Hydrology and Earth System Sciences*, vol. 16, no. 1, pp. 241–254, 2012.

[18] P. C. D. Milly, J. Betancourt, M. Falkenmark et al., "Stationarity is dead: whither water management?," *Science*, vol. 319, no. 5863, pp. 573-574, 2008.

[19] X. Y. Lv, X. Z. Zhang, and J. N. Chen, "The interdecadal variation of advance and retreat of east Asian summer monsoon and their effect on the regional rainfall over China," *Journal of Tropical Meteorology*, vol. 19, no. 4, pp. 340–348, 2013.

[20] H. Liu, T. Zhou, Y. Zhu, and Y. Lin, "The strengthening East Asia summer monsoon since the early 1990s," *Chinese Science Bulletin*, vol. 57, no. 13, pp. 1553–1558, 2012.

[21] M. R. Haylock and C. M. Goodess, "Interannual variability of European extreme winter rainfall and links with mean large-scale circulation," *International Journal of Climatology*, vol. 24, no. 6, pp. 759–776, 2004.

[22] A. Moberg and P. D. Jones, "Trends in indices for extremes in daily temperature and precipitation in central and western Europe, 1901-99," *International Journal of Climatology*, vol. 25, no. 9, pp. 1149–1171, 2005.

[23] C. Svensson, "Empirical orthogonal function analysis of daily rainfall in the upper reaches of the Huai River basin, China," *Theoretical and Applied Climatology*, vol. 62, no. 3-4, pp. 147–161, 1999.

[24] A. K. Smith and H. M. F. Semazzi, "The role of the dominant modes of precipitation variability over Eastern Africa in modulating the hydrology of lake victoria," *Advances in Meteorology*, vol. 2014, Article ID 516762, 11 pages, 2014.

[25] J. R. M. Hosking, "L-moments: analysis and estimation of distributions using linear combinations of order statistics," *Journal of the Royal Statistical Society: Series B (Methodological)*, vol. 52, no. 1, pp. 105–124, 1990.

[26] J. R. M. Hosking and J. R. Wallis, *Regional Frequency Analysis: An Approach Based on L-Moments*, Cambridge University Press, Cambridge, UK, 1997.

[27] C. Cunnane, "Statistical distributions for flood frequency analysis," World Meteorological Orgnization Operational Hydrology Report, No. 33, WMO-No. 718, WMO, Geneva, Switzerland, 1989.

[28] A. R. Rao and K. H. Hamed, *Flood Frequency Analysis*, CRC Press LLC, Boca Raton, FL, USA, 2000.
[29] G. R. North, T. L. Bell, R. F. Cahalan, and F. J. Moeng, "Sampling errors in the estimation of empirical orthogonal functions," *Monthly Weather Review*, vol. 110, no. 7, pp. 699–706, 1982.
[30] V. Semenov and L. Bengtsson, "Secular trends in daily precipitation characteristics: greenhouse gas simulation with a coupled AOGCM," *Climate Dynamics*, vol. 19, no. 2, pp. 123–140, 2002.
[31] X. Zhu, J. He, and Z. Wu, "Meridional seesaw-like distribution of the Meiyu rainfall over the Changjiang-Huaihe River Valley and characteristics in the anomalous climate years," *Chinese Science Bulletin*, vol. 52, no. 17, pp. 2420–2428, 2007.
[32] J. D. Salas and J. Obeysekera, "Revisiting the concepts of return period and risk for nonstationary hydrologic extreme events," *Journal of Hydrologic Engineering*, vol. 19, no. 3, pp. 554–568, 2014.
[33] E. Gilleland and R. W. Katz, "extRemes 2.0: an extreme value analysis package in R," *Journal of Statistical Software*, vol. 72, no. 8, pp. 1–39, 2016.
[34] L. H. Xiong, C. Jiang, T. Du, S. L. Guo, and C.-Y. Xu, "Review on nonstationary hydrological frequency analysis under changing environments," *Journal of Water Resources Research*, vol. 4, no. 4, pp. 310–319, 2015, in Chinese.
[35] A. Cancelliere, "Non stationary analysis of extreme events," *Water Resources Management*, vol. 31, no. 10, pp. 3097–3110, 2017.

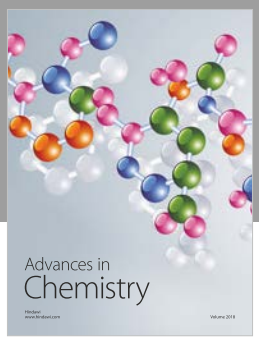

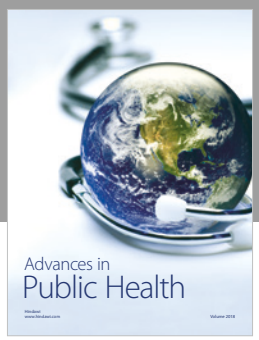

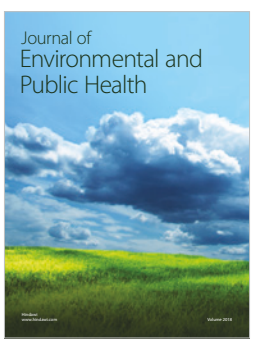

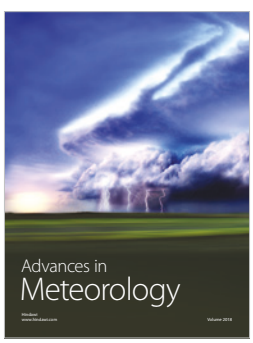

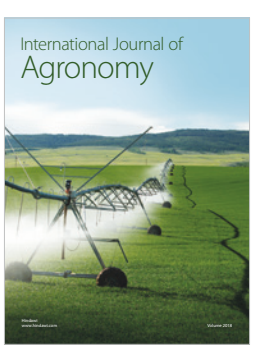

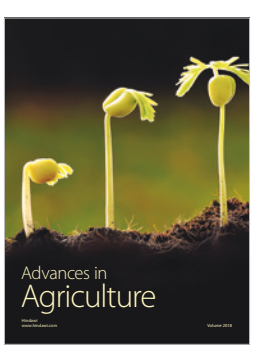

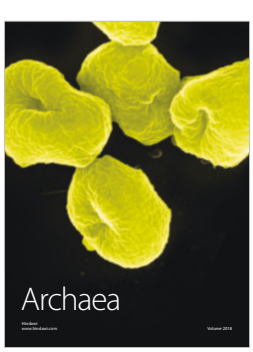

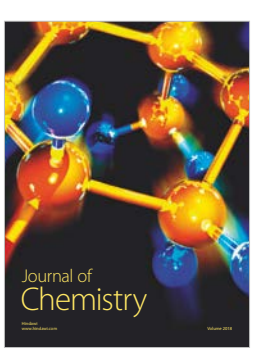


Hindawi

Submit your manuscripts at
www.hindawi.com